Comparison of Thermal Performance for Two Types of ETFP System under Various Operation Schemes

Lingtong Li[1], Zaiguo Fu[1,*], Benxiang Li[2] and Qunzhi Zhu[1]

Abstract: The earth to fluid pipe (ETFP) system has been widely applied to various energy engineering. The numerical model of the heat transfer process in the ETFP system with a shallow-buried horizontal or a deep-buried vertical U-shape pipe adopted in practical engineering was established and the model distinctions were pointed out. The comparison of the thermal performance between the two types of ETFP system under various schemes was conducted on the basis of numerical prediction. The results showed that the thermal parameters of the ETFP system with a shallow-buried horizontal pipe were influenced by the inlet velocity and ground temperature obviously. The variation of the fluid temperature was smooth and the thermal influence zone was limited under the fixed conditions. The proper intermittent operation scheme reduced 53.1% outlet fluid temperature rising. By contrast, the fluid temperature in the ETFP system with a deep-buried vertical U-shape pipe varied dramatically with the operation conditions. The intermittent operation scheme with a relatively short interval led to a less temperature fluctuation of soil around the pipe. The intermittent scheme is beneficial to the recovery of the thermal condition of soil around the U-shape pipe. These results indicated a stark difference in thermal performance between the two types of system. The study can provide guidance for the selection and operation of ETFP system in practical heat exchange engineering.

Keywords: Heat transfer, buried pipe, ETFP, heat exchange, numerical simulation.

1 Introduction

The earth to fluid pipe (ETFP) system can implement the heat exchange between the earth and the fluids in the buried pipe [Soni, Pandey and Bartaria (2015); Florides and Kalogirou (2007)]. The fluids (gas or liquid) are determined by the engineering requirement and the acceptable economic cost. They are introduced into the buried pipe by pumps or

[1] College of Energy and Mechanical Engineering, Shanghai University of Electric Power, Shanghai, 200090, China.
[2] Sino-Pipeline International Co., Ltd., Zhejiang, 312000, China.
* Corresponding Author: Zaiguo Fu. Email: fuzaiguo2009@hotmail.com.
Received: 30 November 2019; Accepted: 20 January 2020.

compressors and generate convective heat transfer with the inner wall during their flow or stay in the pipe. The pipe wall, coating, backfill materials and soil surrounding the pipe conduct heat continuously. Therefore, this ETFP system is a complicated heat exchange system composed of multiple heat transfer processes which might be affected by various thermal conditions [Rashidi, Esfahani and Karimi (2018)].

There are wide applications of the similar ETFP system with underground heat exchanger. Ozgener et al. [Ozgener, Ozgener and Tester (2013)] built a model to predict daily soil temperatures depending on depth and time. The soil temperature measurements were made on an earth to air heat exchanger (EAHE) system to analyze the effect of solar fluctuations. Barakat et al. [Barakat, Ramzy, Hamed et al. (2016)] proposed an EAHE cooling system and analyzed the feasibility of its application for gas turbine to cool the inlet air by numerical calculation. It was evident that the caused inlet air cooling could increase the output power of gas turbine and the thermal efficiency. Rodrigues et al. [Rodrigues, Brum, Vaz et al. (2015)] have studied the influence of geometrical configurations of an EAHE system in built environment and found that the increase of the number of ducts improved the thermal performance of the system for air cooling and heating. Misra et al. [Misra, Bansal, Agrawal et al. (2013)] evaluated the thermal performance of earth air tunnel heat exchanger (EATHE) in winter season. A rise of 19.6 K is obtained for air passing through the EATHE system under steady state condition.

Additionally, the earth to air or water heat exchanger (EAWHE) has also been adopted and studied in the field of geothermal utilization [Kayaci and Demir (2018); Liu, Xiao, Inthavong et al. (2015); Pei and Zhang (2016)]. Kayaci et al. [Kayaci and Demir (2018)] pointed out that an underground heat exchanger is the most important part of a ground source heat pump. They investigated the influence of buried depth, distance between pipes and surface effects on soil temperature. Moreover, there are many applications of this similar ETFP system in developing solar energy for thermal storage and solar regeneration [Pavlov and Olesen (2011); Miglani, Orehounig and Carmeliet (2017, 2018); Kadir, Omer, Kemal et al. (2011); Arvind and Tiwari (2010, 2011)]. The system usually integrates solar thermal collectors and ground source heat pumps via underground borehole heat exchanger.

Due to these wide applications of system with underground heat exchanger in various fields, it is essential to study the heat transfer process between surrounding soil and the flowing fluid in the system. In order to generalize the system, we redefined it as ETFP in previous study to incorporate the abovementioned EAHE, EATHE and EAWHE systems [Fu, Li, Zhang et al. (2018)]. It covers the underground heat exchanger system using tunnel [Ozgener (2011)] or buried pipe, with gas or liquid as working medium. It can be applied in not only fluid cooling but also fluid heating via horizontal and vertical heat exchangers. Thus, ETFP system has a wider application scope than those systems listed above.

Presently, many researchers have done some numerical research to investigate the thermal performance of ETFP system. Belatrache et al. [Belatrache, Bentouba and Bourouis (2017)] modeled and simulated a shallow-buried horizontal ETFP system based on the energy balance equations by assuming that the soil temperature is constant. The appropriate depth of buried pipe and the effects of other parameters, such as pipe length, pipe radius and air velocity in the pipe were investigated. Bisoniya et al. [Bisoniya, Kumar and Baredar (2015)] developed a steady state, three-dimensional (3D) model of the pipe in an ETFP system to investigate the annual thermal performance based on computational fluid dynamics (CFD) software. In the calculation, the soil temperature was given and taken as boundary conditions. The thermal influenced soil domain was not taken into account. Ramirez-Davila et al. [Ramirez-Davila, Xaman, Arce et al. (2014)] presented a numerical analysis of a 2D conjugate heat transfer between the buried pipe and soil under various climate conditions corresponding to three cities in Mexico. The cross section of pipe was modeled as a square cross section and a rectangular zone was taken as calculation domain. Misra et al. [Misra, Bansal, Agrawal et al. (2013); Bansal, Mishra, Agrawal et al. (2012)] carried out a 3D transient CFD analysis of a shallow-buried horizontal ETFP system. They assumed that the outer surface of the surrounding soil cylinder with a diameter 10 times the pipe was at a constant temperature and employed it as the soil thermal boundary in calculation. Mathur et al. [Mathur, Mathur, Agrawal et al. (2017)] modeled a straight and new spiral shaped ETFP system. A cubic zone was taken as the calculation domain and the boundaries in the soil environment were treated as fixed temperature surfaces.

About the vertical deep-buried ETFP system, some researchers have established the thermal model of the U-tubes and investigated the effects of pipe spacing, pipe diameter, inlet temperature and soil condition etc. [Zhang, Huang, Wang et al. (2014); Wu, Liu, Lu et al. (2017); Babak and Ergin (2017)]. The results indicated that the reasonable spacing could avoid the mutual interference and the raising inlet fluid temperature could increase the temperature difference between inlet and outlet. The larger spacing and diameter of U-tube, the higher efficiency of the thermal conversion could be obtained. The specific heat capacity of the backfill material could be ignored. Moreover, Zhang et al. [Zhang, Zhang and Huang (2016)] and Ruiz-Calvo et al. [Ruiz-Calvo, Rosa, Acuna et al. (2015)] investigated the operation process of the vertical ground heat exchanger and found the outlet temperature became stable after running of several hours and its rising was limited after short-term operation. Besides, some researchers simulated the ETFP system by adopting the concept of thermal influence zone to ascertain the range of disturbed soil and forecast the interaction between buried pipe and soil successfully [Cui and Zhang (2004); Yu, Li, Zhang et al. (2010); Xu, Yu, Zhang et al. (2010); Li, Sheng, Jin et al. (2010); Fu, Yu, Zhu et al. (2012)].

It is evident from these studies that numerical calculation is an effective method to simulate the heat exchange between earth and fluid via buried pipe or excavating tunnel in ETFP system and to predict the system's thermal performance. Most of the aforementioned researchers studied the thermal performance of the similar ETFP system by treating it as a unique type [Belatrache, Bentouba and Bourouis (2017); Bisoniya, Kumar and Baredar (2015); Misra, Bansal, Agrawal et al. (2013); Bansal, Misra, Agrawal et al. (2013);

Wang, Sun, Gong et al. (2018); Wang, Sun and Yu (2017)]. Few studies have addressed the similarities and differences of the thermal performances for various types of ETFP system operated under different conditions.

The main purpose of this study is to conduct a numerical investigation on the difference of thermal performance between two types of ETFP system. The shallow-buried horizontal and deep-buried vertical ETFP systems are differentiated. Their characteristics and thermal performances under various operation schemes are compared specially. The present paper is arranged as follows. Firstly, the physical model of the heat transfer process in the ETFP system developed for air cooling and heat storage is established. The employed numerical procedure is introduced. Secondly, on the basis of the validation of the numerical model and method, the thermal performances of the two types of ETFP system including the variations of the fluid and soil temperature under various operation schemes were investigated compared. Finally, the conclusions on the distinction of the characteristics and performance between the two types of system were given.

2 Modeling and numerical procedure

2.1 Geometric model

Two types of physical model of the ETFP system were classified according to the heat flux conditions around the buried pipe in our previous work [Fu, Li, Zhang et al. (2018)]. Accordingly, we establish the geometric model of the two types of the ETFP system developed for the fluid cooling and heat storage engineering as shown in Fig. 1.

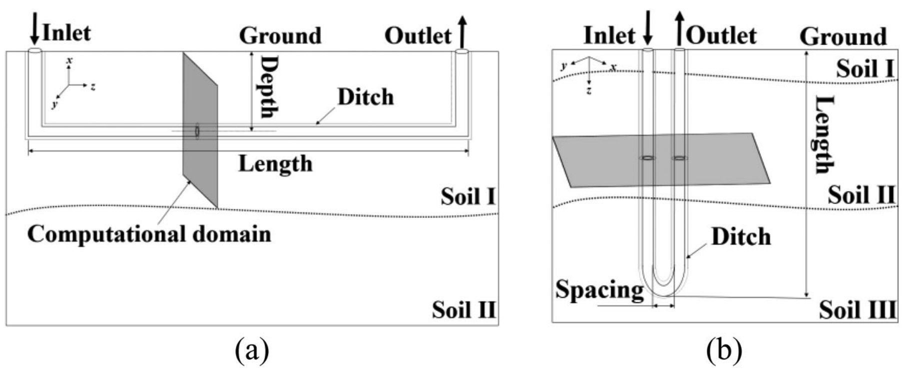

Figure 1: Sketch of the ETFP system with a: (a) shallow-buried horizontal pipe and (b) deep-buried vertical U-shape pipe

Fig. 1(a) shows the system with a shallow-buried horizontal pipe. The entered air gets cooling when flows through the pipe. The soil thermal conditions around the pipe at any certain axial position are non-uniform circumferential due to the asymmetric boundaries. The length and diameter of the pipe are 50 m and 0.3 m respectively. The buried depth is 1.5 m. The direction along the pipe axis is defined as *z*. The pipe is arranged in a ditch denoted by the surrounding lines. The size of the cross section (*x*-*y* plane) of the system is 10 m×10 m. It is denoted by the grey region.

Fig. 1(b) shows the system with a deep-buried vertical U-shape pipe. The initial soil thermal conditions around the pipe at any certain axial position are uniform circumferential. The entered hot water gets cooling when flows through the U-shape pipe and the heat is stored in the surrounding soils. The depth and diameter of the U-shape pipe are 50 m and 0.1 m respectively. The pipe spacing is 0.5 m. The direction along pipe axis is also defined as *z*. The pipe is set in the borehole denoted by the surrounding lines. The size of the cross section (*x*-*y* plane) of the system is also 10 m×10 m.

The surrounding soils in the range with the height of 0-5 m and 5-10 m are clay and mudstone as soils I and II in Fig. 1, respectively. The gravel sand distributes below the mudstone layer as soil III.

2.2 Mathematical model

The heat transfer process in the ETFP system mainly contains the convective heat transfer of fluids in the pipe and the heat conduction outside the pipe. The balance of heat flux is used to couple the convective heat transfer in the pipe and the soil heat conduction. The following assumptions are invoked to simplify the numerical calculation of the heat transfer process.

(1) The temperatures of fluid are assumed to be uniform without stratification in the buried pipe, i.e., the temperatures are only a function of time and the axial location.

(2) The soil is isotropy and the effect of moisture migration in soil on temperature field is ignored. The soil and fluid properties are independent of temperature.

(3) The effect of radiation on the soil surface is ignored.

(4) The thermal influence of the system is limited in a finite zone. The rectangular cross section perpendicular to the pipe axis denotes the range of influence at a fixed axial position.

2.2.1 Governing equation

Based on the above assumptions, the coupling fluid flow and heat transfer process for both types of ETFP system is considered as one-dimensional in pipe and two-dimensional in the calculation soil domain. The equations of mass conservation, momentum conservation and energy conservation of the fluid flow in the buried pipe are expressed as follows:

$$\frac{\partial}{\partial \tau}(\rho A)+\frac{\partial}{\partial \mathrm{z}}(\rho V A)=0 \tag{1}$$

$$\frac{\partial V}{\partial \tau}+V\frac{\partial V}{\partial \mathrm{z}}=-\mathrm{g}\sin\alpha-\frac{1}{\rho}\frac{\partial P}{\partial \mathrm{z}}-\frac{f}{D}\frac{V^2}{2} \tag{2}$$

$$c_P \frac{dT_{\mathrm{f}}}{d\tau} - \frac{T_f}{\rho}\beta\frac{dP}{d\tau} - \frac{fV^3}{2D} = -\frac{4q}{\rho D} \tag{3}$$

where, ρ is the fluid density. V is the average velocity of the fluid flow in the pipe. A is the cross-section area of pipe. τ is time. P is the average pressure along the pipe. f is Darcy friction coefficient. D is the inner diameter of pipe. β is the expansion coefficient of the fluid. The angle of α in Eq. (2) equals 90° and 0° for the ETFP system with horizontal and vertical pipe, respectively. c_p denotes the heat capacity of fluid. T_f is the fluid temperature. q denotes the axial heat flux of the fluid flow. It is equal to the exchanged heat between the fluid flow and pipe wall on the cross section of the pipe. In Eq. (3), the first term is the absorbed or released heat via temperature variation. The second term and the third term denote the heat change caused by fluid expansion and friction loss respectively. The right side of the equation stands for the released heat from the pipe internal wall.

The governing equation of heat conduction in surrounding multilayer materials of the pipe including the pipe wall, protective covering and backfill layer in the ditch or borehole is presented in the polar coordinates as follows:

$$\rho_i c_i \frac{\partial T_i}{\partial \tau} = \frac{1}{r}\frac{\partial}{\partial r}\left(\lambda_i r \frac{\partial T_i}{\partial r}\right) + \frac{1}{r^2}\frac{\partial}{\partial \theta}\left(\lambda_i \frac{\partial T_i}{\partial \theta}\right) \; i = 1, 2, 3 \tag{4}$$

The governing equation of heat conduction in surrounding soils of the pipe is given as:

$$\rho_s c_s \frac{\partial T_s}{\partial \tau} = \frac{\partial}{\partial x}\left(\lambda_s \frac{\partial T_s}{\partial x}\right) + \frac{\partial}{\partial y}\left(\lambda_s \frac{\partial T_s}{\partial y}\right) \tag{5}$$

In Eqs. (4) and (5), ρ_i and ρ_s are the densities of multilayer materials and soil respectively. i=1, 2, 3 corresponds to pipe wall, protective covering and backfill layer, respectively. c_i and c_s denote the heat capacity of multilayer materials and soil respectively. T_i and T_s are the temperatures of multilayer materials and soil respectively. r is the radial direction and θ is the circumferential direction. λ_i and λ_s is the thermal conductivity of multilayer material and soil respectively. x and y are the two directions of the straight side of the rectangular calculation domain, respectively.

2.2.2 Boundary conditions

The ground surface is set as the Robin boundary condition, it is expressed as:

$$\lambda_s \frac{\partial T_s}{\partial y} = \alpha_a (T_a - T_f) \tag{6}$$

Other thermal boundaries are different for the two types ETFP system. For the shallow-buried horizontal ETFP system, they are expressed as follows.

$$\text{At } x = 0 \text{ or } L, \frac{\partial \mathrm{T_s}}{\partial \mathrm{x}} = 0 \tag{7}$$

$$\text{At } y = H, \ \mathrm{T_s}{=}\mathrm{T_c} \tag{8}$$

For the deep-buried vertical pipe, the boundaries are expressed as follows.

$$\text{At } x = 0 \text{ or } L, \ \frac{\partial T_s}{\partial x} = 0 \tag{9}$$

$$\text{At } y = 0 \text{ or } H, \ \frac{\partial T_s}{\partial y} = 0 \tag{10}$$

$$\text{At } z = h_1 \text{ or } h_2, \ T_s{=}T_c \tag{11}$$

$$\text{For both types, at the pipe wall, } \lambda_\mathrm{p} \frac{\partial T_p}{\partial r} {=} \alpha_\mathrm{f} (T_f - T_p) \tag{12}$$

In Eqs. (6-12), L and H stand for the size of the thermal influencing distances in x, y direction respectively. h_1 and h_2 stand for the certain soil layer heights. T_c denotes a certain constant temperature. α_a, α_f denotes the convective heat transfer coefficients of the air flow over the ground and of the fluid flow in pipe, respectively. They can be derived from the Nusselt number calculated by empirical formulas, such as Gnilinski and Dittus-Boelter equations [Bergman, Lavine, Incropera et al. (2017)] etc., according to the flow regime and fluid type.

2.2.3 Other parameters

The thermophysical parameters of fluids and soils adopted are listed in Tab. 1.

Table 1: Thermophysical parameters of various materials [Barakat, Ramzy, Hamed et al. (2016); Cui and Zhang (2004); Fu, Li, Zhang et al. (2018)]

Material	Density (kg/m^3)	Thermal conductivity W/(m·K)	Specific heat capacity J/(kg·K)
Air	1.092	0.0265	1013
Water	998	0.599	4183
Clay	1600	1.4	1041
Mudstone	1800	1.2	1000
Gravel	2000	2.0	750

2.3 Numerical procedure

2.3.1 Discrete grids

The grids of the buried pipe are generated as equally spaced pipe sections along z direction. The numerical calculation starts at the inlet and ends at the outlet. In the present study, uniform grids with the length of 5 m are adopted to obtain the fluid temperature distribution along the pipe axis. The Delaunay triangulation method is adopted to generate unstructured grids for soils in the calculation domain, i.e., the thermal influence zone automatically. The structured quadrilateral grids in the polar coordinate system are generated for the multilayer materials around the pipe. Denser grids are generated in the region in the vicinity of pipe without overlapping each other since the temperature gradient is greater there. In the two-dimensional thermal influence zone perpendicular to the pipe axis, the rational grid density with 40 nodes along the x, y directions are determined after grid independence validation.

2.3.2 Numerical method

The governing equations for the fluid flow and heat conduction are discretized in different ways. Finite volume method was employed to discretize the equations of heat conduction for multilayer materials and soil. Finite difference method was adopted to solve the fluid flow problem. The soil temperature and fluid temperature were solved simultaneously by iterative solution using the coupling relationship between the interfaces of pipe and soil in thermal influence zone. In the present study, an implicit method is used for time discretization and a second-order discretization of other terms is used. The validation of this procedure is presented in the following section.

3 Results and discussions

The thermal performance including the temperature drop of the fluid in the buried pipe and the soil temperature variation of the ETFP system developed for the air cooling and heat storage engineering are predicted and compared on the basis of a validation of the numerical model and procedure. The distinctions of the performance under continuous and intermittent operation schemes are analyzed for the two types of ETFP system specially.

3.1 Model validation

To validate the developed numerical model and the numerical method in present work, the calculation was conducted under the same conditions as the literature by Bansal et al. [Bansal, Mishra, Agrawal et al. (2012)] listed in Tabs. 2 and 3. The results of the predicted temperature drop in an ETFP system with a horizontal buried pipe under various thermal influencing distances are shown with the actual experimental data in Fig. 2. Moreover, we carried out a 3D numerical simulation of this ETFP system to further validate the reliability and accuracy of the numerical results. The software of FLUENT 15.0, as a widely applied CFD tool to analyze the complicated fluid flow and heat transfer process in engineering, was used. To reduce the computational time, half of the 3D geometric model of the ETFP system was established according to the aforementioned literature as shown in Fig. 3.

The model is cubic and with the size of 23.42 m×10.7 m×5 m (x×y×z, x denotes the length along the axial direction of pipe; y is the vertical buried depth from the ground; z corresponds to the horizontal distance in the cross section of pipe). It is discretized by

Table 2: Thermophysical properties of materials and velocity [Bansal, Mishra, Agrawal et al. (2012)]

Material	Density (kg/m^3)	Thermal conductivity W/(m·K)	Specific heat capacity J/(kg·K)	Velocity (m/s)
Air	1.225	0.0242	1006	5
Soil	2050	1.16	1840	–
PVC	1380	0.16	900	–

Table 3: Geometric dimensions of ETFP system [Bansal, Mishra, Agrawal et al. (2012)]

Experimental parameters	Value (in m)
Pipe length	23.42
Inner pipe diameter	0.15
Buried depth	2.7

62.2 million cells. The centerline of the buried pipe is located from (0, −2.7, 0) to (23.42, −2.7, 0). The diameter of the pipe is 0.15 m. The pipe wall is composed of PVC material and 0.005 m thick. The soil fills the rest of region and the average temperature around the buried depth is 299.9 K. The inlet air temperature is 311.4 K. The pipe wall is thermal coupled. The turbulent model of Realizable *k-ε* is selected for turbulence calculation.

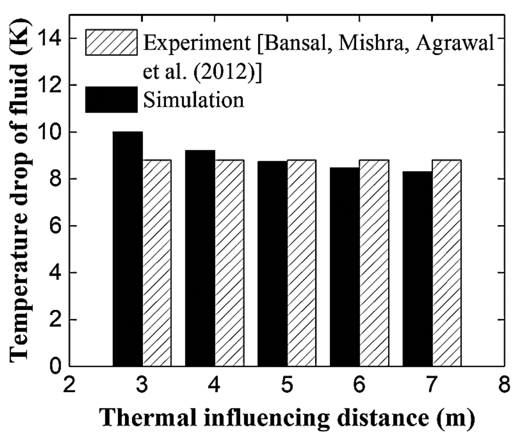

Figure 2: Comparison of the simulation results with experimental results under various thermal influencing distances

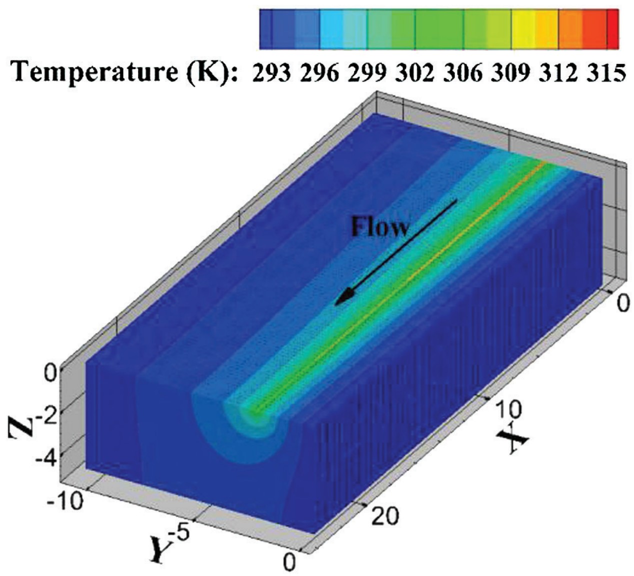

Figure 3: The 3D geometric model of an actual ETFP system

In Fig. 2, the simulation results show that when the thermal influencing distance of the buried pipe is set as 5 m, the calculated temperature drop of air flow has a minimum difference with the experimental result. As the distance less than 5 m, the soil beyond the thermal influence zone still have a significant impact on the flow temperature in pipe. Whereas when the selected distance of thermal influence zone is more than 5 m, the effect of the redundant computation domain of soil is less than 1 K of air temperature drop but increases the computational complexity. The difference of the temperature drop between the simulation results and the experimental results is 0.08 K.

In Fig. 3, the air temperature is found to descend obviously along the flow direction. The coupled convection heat transfer integrated with the fluid flow in the pipe is indicated to be captured by the 3D simulation successfully. From the head face of the model, i.e., the first cross section of buried pipe, we can see that the thermal contours around the pipe are quasi-circular. Thermal influencing distance is limited in this quasi-circular region and in 4 m along z direction. The maximum temperature difference of the soils outside the thermal influence zone is in 1 K based on the detailed examination of numerical results.

Fig. 4 shows the calculated results of the temperature variation along the air flow in the buried pipe by the 3D simulation and by the adopted method in the present study along with the measured value in the actual ETFP system reported in Bansal et al. [Bansal, Mishra, Agrawal et al. (2012)]. By comparison, it can be found that the calculated result by the present method approximates the calculated result by the 3D simulation. They also agree well with the experimental value. The maximum deviation is 1.1 K relative to the measurements for the 3D calculations. It becomes smaller for the present calculation. It

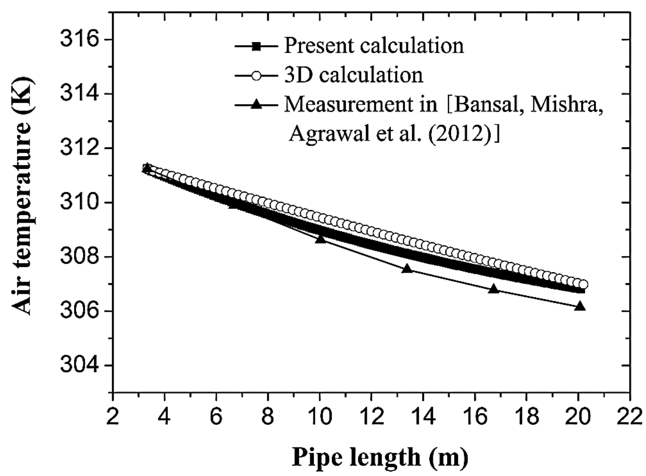

Figure 4: Comparison of the calculated temperature variation with the measured value of an actual ETFP system

should be noted that, due to the exposure of the inlet and outlet to the environment in the actual ETFP system, the inlet and outlet temperatures respectively reported are not used to be compared. However, the total temperature drop of 8.8 K along the pipe flow can be compared via the calculation on the basis of the total pipe length. The above comparison results indicate the reliability of the present method to solve the coupling problem of fluid flow and heat transfer in ETFP system.

3.2 A horizontal shallow-buried system

3.2.1 Fluid temperature variation

The air velocity in the ETFP system with a shallow-buried horizontal pipe is set from 1.0 m/s to 4.0 m/s to investigate the fluid temperature variation under various operation flow rates. Moreover, the air flow is set to be operated in two intermittent schemes with different intervals as well as in a continuous scheme. Fig. 5 shows the fluid temperature drop along the pipe after continuous running of 0.5 h and 24 h, respectively. Fig. 6 shows the variation of the outlet fluid temperature under the continuous and intermittent schemes. Under the normal scheme, the system is running continuously. The scheme of normal-stop 1 corresponds to a running of 8 hours and a stop of following 16 hours in one day. The scheme of normal-stop 2 corresponds to a running of 48 hours (two days) and a stop of following 48 hours (two days).

From Fig. 5, it can be seen that the air temperature declines along the pipe flow. This indicates the excellent cooling effect of the ETFP system. In addition, the temperature drop decreases with the increase of air velocity, which can be explained by the relatively short standing time of hot air corresponding to a large velocity. On the other side, the enhanced heat exchange coefficient between the air flow and pipe wall affected by the

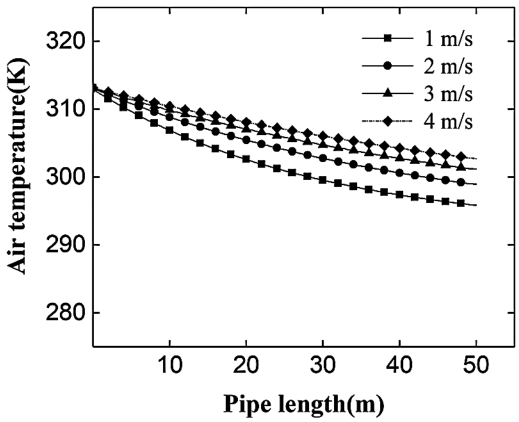

(a)

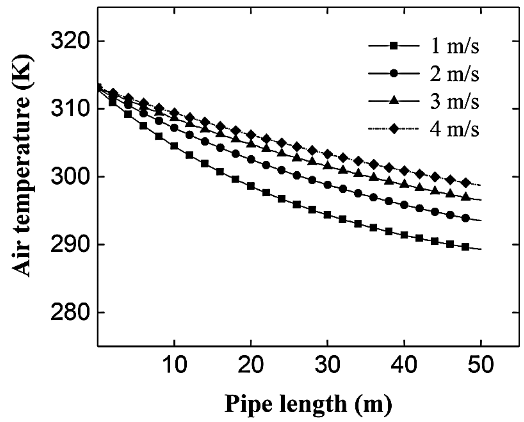

(b)

Figure 5: Variation of air temperature along pipe after (a) 0.5 h and (b) 24 h under the normal scheme

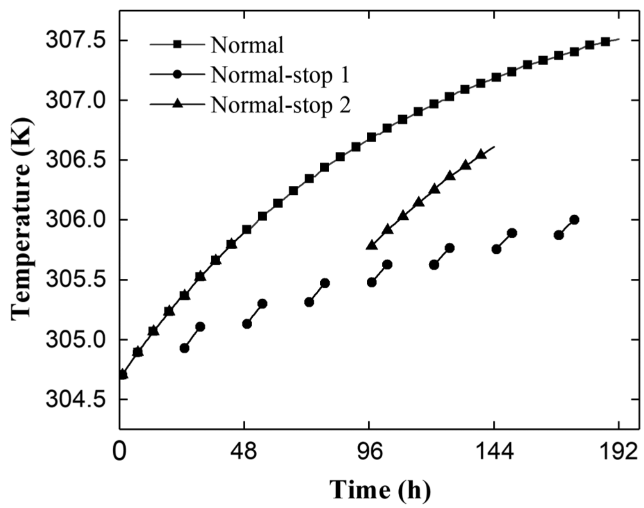

Figure 6: Variation of outlet fluid temperature under various operation schemes

increasing velocity is limited. The comparison between Figs. 5(a) and 5(b) reveal that the variation of air temperature is unsteady and tends to be stable with the continuous operation. The temperature drop after 0.5 h operation is a little larger that after 24 h operation due to the reduced temperature difference between the soil and the air flow. The thermal inertia of soils makes against the air cooling.

The shallow-buried horizontal pipe is common in the fields of ventilation system in residences and inlet air cooling for gas-turbine. The results on the variation of outlet fluid temperature under three operation schemes for 192 h are shown in Fig. 6. It is clearly that the continuous operation as the normal scheme results in the temperature increasing in 192 h with the final outlet fluid temperature as 307.5 K. The discontinuous operation as normal-stop 1 and normal-stop 2 can make use of the thermal recovery of soil and provide lower temperature during running process. For the normal-stop 1 scheme, the outlet fluid temperature is 1.2 K and 0.3 K lower than the normal and normal-stop 2 schemes respectively at 96 h. After 192 h running, the final temperature drops are 5.5 K, 7.0 K and 6.4 K of normal, normal-stop 1 and normal-stop 2 schemes respectively. Moreover, when compared with normal scheme, the intermittent scheme as normal-stop 1 and normal-stop 2 can reduce 53.1% and 32.1% temperature rising. As a result, the intermittent operation can keep the outlet temperature lower in a long-term operation because the fully use of the thermal recovery of soil. The system under normal-stop 1 scheme can have a lowest outlet fluid temperature among three operation schemes.

3.2.2 Soil temperature variation

The soil temperature at a certain cross section is investigated to examine the effects of ground condition. The fluid temperature of 313.2 K is chosen. The convective heat transfer coefficient between the pipe wall and air flow α_a is 20 W/(m^2·K). Fig. 7 shows the soil temperature in a horizontal line under various climate conditions (expressed by the ambient air temperature, T_a). The line is on the unilateral side of pipe and through its center point. Fig. 8 shows the heat fluxes of the pipe wall. Fig. 9 shows the variation of the soil temperature at the location of 1 m away from the pipe wall along x direction under the intermittent schemes.

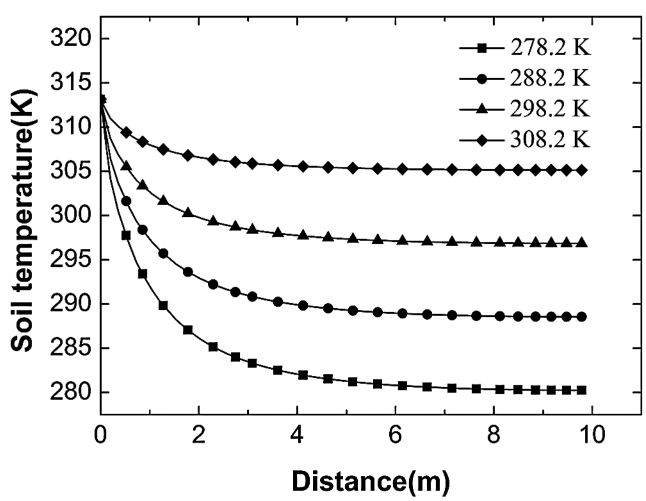

Figure 7: Temperature distribution on the unilateral side of pipe

From Fig. 7, it can be seen that the thermal influencing distance is enlarged from 4 m to 6 m predicted by the mutational curve slopes under T_a of 308.2 K and 278.2 K with the decrease of ambient air temperature, i.e., the increase of temperature difference between T_f and T_a.

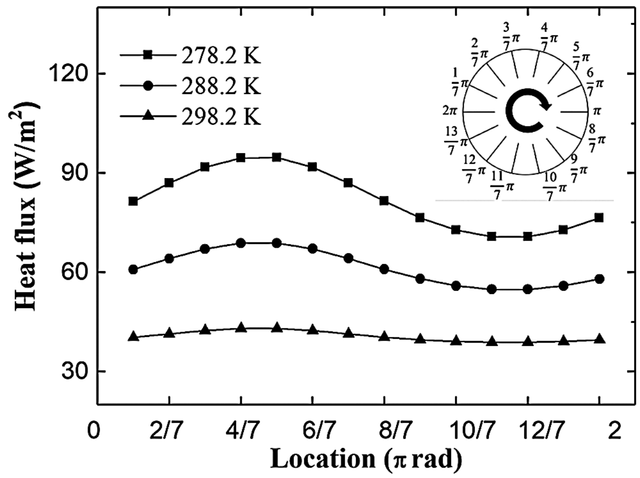

Figure 8: Heat flux along the circumferential direction of pipe wall

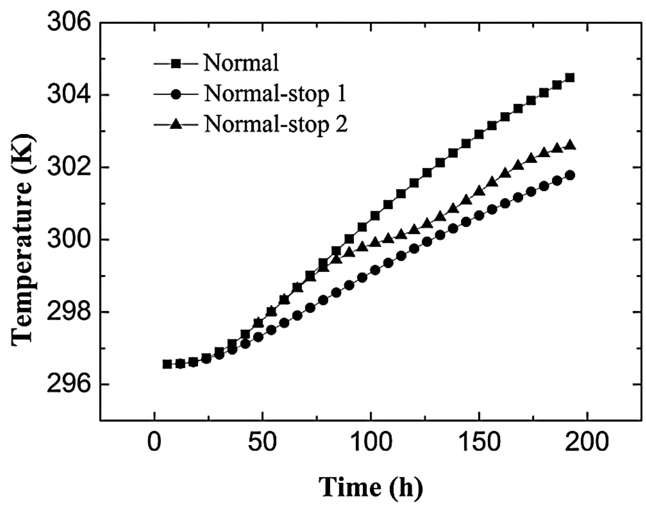

Figure 9: Soil temperature variation in the ETFP system under various operation schemes

However, they are all limited in the thermal influence zone, which has a unilateral length of 10 m. This calculated result agrees well with the reported result in Cui et al. [Cui and Zhang (2004)] using the same thermal parameters. This also validates the reliability of the proposed method to set a thermal influence zone.

In Fig. 8, the elliptical, non-round contour line of soil temperature around pipe at two conditions is obvious. Due to the effect of the ambient air temperature, the part of soil above the pipe in the case of T_a=278.2 K is disturbed severely by the buried pipe. Whereas in the case of T_a=298.2 K the part below the pipe is disturbed severely. The non-uniform local heat flux along the circumferential pipe wall indicates the various thermal conditions of the surrounding soil, which can be described by the model of type I emphasizing the non-uniform thermal conditions. In the figure, the abscissa represents the location on the pipe wall count clockwise from the horizontal right position. The larger heat flux is observed for the case of lower T_a. The reason is same as the explanation for the phenomena of different thermal influencing distance shown in Fig. 7.

It is found from Fig. 9 that the soil temperature increases with the time during the operating period. By comparison, the normal scheme results in an increase of 8 K. However, the normal-stop 1 and normal-stop 2 schemes cause relatively small rises in soil temperature. The scheme of normal-stop 1 with a short interval can suppress the temperature rise of the soil surrounding the pipe in the ETFP system. In other word, the intermittent scheme with a relatively long stop time is beneficial to the recovery of soil temperature. Thus, a relatively large temperature difference between the fluid and soil can be attained. It makes a good cooling performance.

3.3 A vertical deep-buried system

3.3.1 Effects of pipe spacing

A deep-buried vertical U-shape pipe with an identical diameter of 0.1 m at conditions of various spacing of 0.5 m, 1 m, 2 m, various fluid temperatures of 313.2 K, 353.2 K, initial soil temperature of 288.2 K was operated in the heat storage and release process of an ETFP system. The initial temperature of pipe wall was assumed to be same as the fluid temperature and the multilayer materials were assumed to be the surrounding soil for simplification. Fig. 10 shows the mutual thermal effects of double pipes at three spacing and two fluid temperatures on the soil temperature fields after running 7 days. The fluid temperature flowing in the double pipes is fixed at 353.2 K in Figs. 10(b)-10(d). In Fig. 10, the demonstrated soil range is selected to be a relatively small region for depicting the temperature contours close to the pipe clearly.

From Fig. 10(a), it can be seen that the pipe with the high-temperature fluids dominates the thermal influence zone and the mutual effect is limited. The thermal influence zone is finite when compared to the two pipes with high-temperature fluids of 353.2 K as shown in Fig. 10(b). It also can be seen in Figs. 10(b)-10(d) that with the increase of the spacing between pipes, the mutual effect between pipes becomes weak. The isothermal lines are independent for the case of 2 m spacing in the temperature range from 313.2 K to 353.2 K. The interesting thing is that the shape of isothermal line at the location 0.5 m away from pipe for the case of 0.5 m spacing is quasi-circular. However, for the case of 1 m, the shape is elliptic and the mutual effect between double pipes in horizontal direction is severe. According to the requirement of heat storage, the concentrated heated region caused by small spacing is more applicable.

3.3.2 Soil temperature variation

Figs. 11(a) and 11(b) show the temperature distribution in a horizontal and a vertical line respectively to demonstrate the evolution of the thermal influencing distance under all

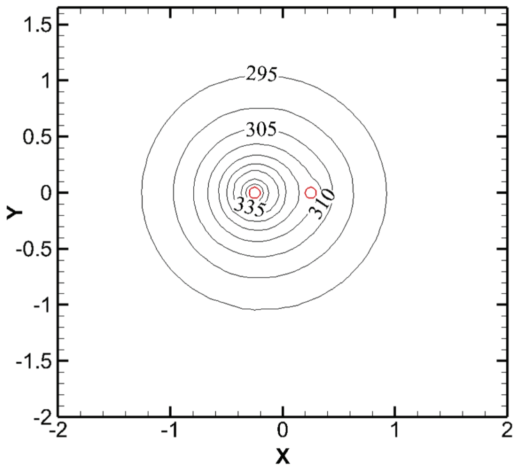

(a)

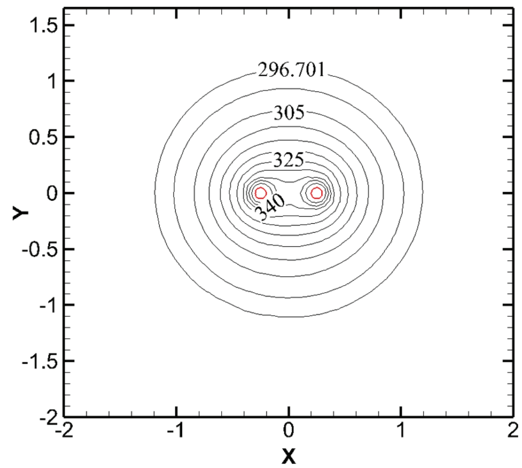

(b)

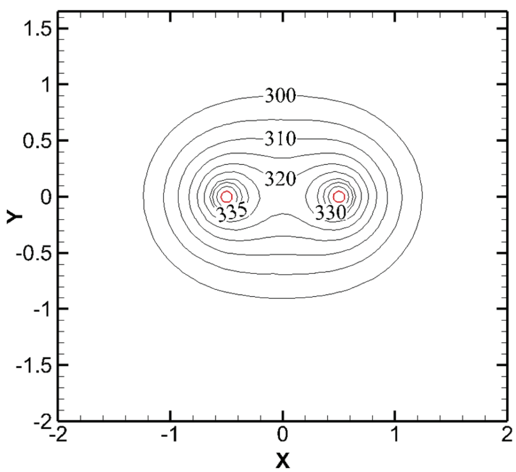

(c)

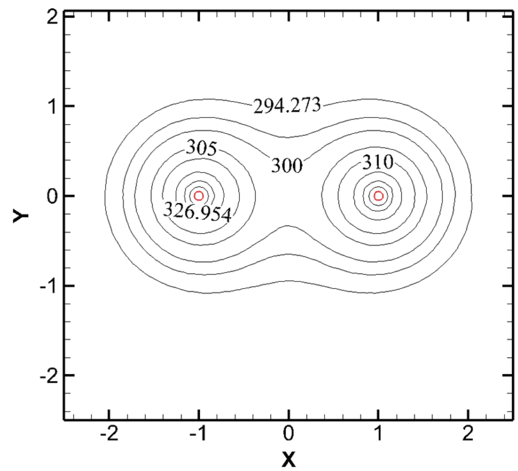

(d)

Figure 10: Mutual thermal effect of double pipes with (a) different fluid temperatures at 0.5 m spacing and with a spacing of (b) 0.5 m (c) 1 m (d) 2 m under same fluid temperatures

operating conditions. The two lines originate from the center point between the double pipes to the boundary of computational domain. In Fig. 11, Condition A represents that the temperatures of double pipes are same and 313.2 K. Condition B indicates the temperatures are 353.2 K and 313.2 K respectively. Condition C corresponds that the temperatures are both 353.2 K. The numbers following the Conditions A, B and C stand for the spacing between the double pipes.

In Fig. 11, it is observed that the thermal influencing distance in the horizontal line is larger than that in the vertical line for the studied case. However, in the practical heat storage

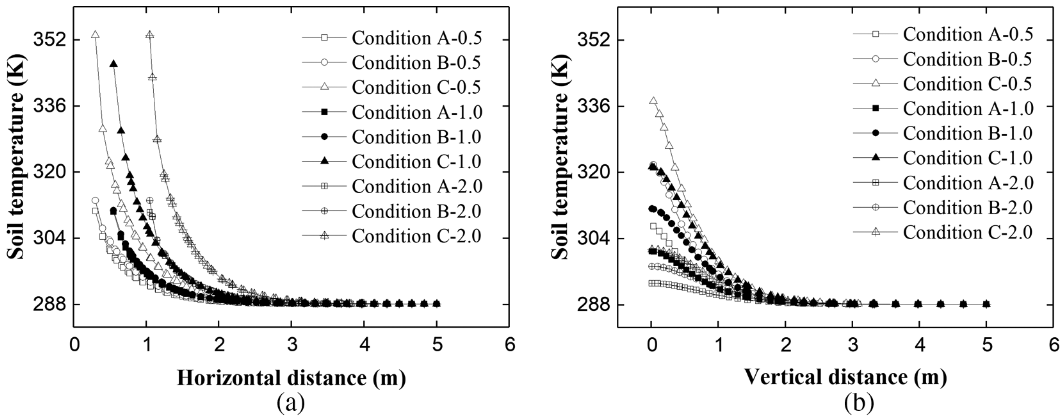

Figure 11: Temperature distribution in a (a) horizontal and a (b) vertical line around pipes

engineering, the adopted pipe group may cause the uniform thermal influencing distance around the pipes in the two directions due to the equal setting of pipes. Moreover, it is drawn that the higher temperature of the inserted fluid in the pipe is set, the richer heat stored in the vicinity of pipes is obtained. This is convenient for the quick operation of heat storage and release.

As for the vertical U-shape pipe, three operation schemes are also arranged to compare the thermal performance of the system. The three operation schemes are also set as normal, normal-stop 1 and normal-stop 2, which is same as the Section 3.2.1. Fig. 12 shows the horizontal thermal influencing distance of the double pipes and the monitored temperature at the fixed center point between the double pipes at conditions of two-type soil, fluid temperature of 353.2 K and spacing of 0.5 m under three operation schemes in 192 h.

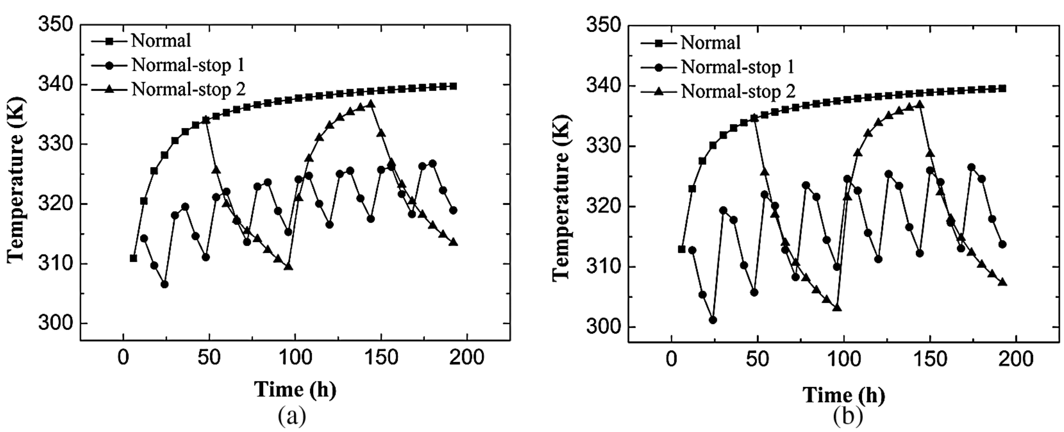

Figure 12: Soil temperature variation in the (a) clay and (b) gravel range

The vertical U-shape pipe is common in the fields of ground source heat pump. As for the different supply form by heat source, the different operation schemes and soil type are needed to be proposed and analyzed. Fig. 12 provides the results of the soil temperature variation in two kinds of soil under different operation schemes. As the gravel has a higher thermal diffusion coefficient than the clay, the temperature fluctuation of gravel is more obvious than clay especially for the normal-stop 1 scheme. By comparing three operation schemes, it is clearly that under continuous operation, the soil temperature increasing continuously while the temperature fluctuation only exists under intermittent operation schemes. Moreover, the normal-stop 1 scheme with a relatively shorter stop interval can store heat effectively in both kinds of soil and keep a large temperature difference with the fluid to enhance heat exchange in 192 h.

3.3.3 Fluid temperature variation

Fig. 13 shows the variation of outlet fluid temperature under three operation schemes. Under the normal scheme, the outlet fluid temperature continuously increases in 192 h and reaches to 346.5 K while the inlet fluid temperature keeps 353.2 K. The temperature drop is 6.6 K between the inlet and outlet fluid temperatures. Under the normal-stop 1 scheme, the temperature is 346.3 K at the end of 192 h for the shorter running time and longer stop time. In normal-stop 2 scheme, the temperature is 346.2 K after 192 h, which is lower 0.3 K and 0.1 K than the temperature under normal and normal-stop 1 schemes respectively. Therefore, when compared with normal scheme, the intermittent operation under normal-stop 1 and normal-stop 2 schemes can reduce 17.4% and 29.5% temperature rising.

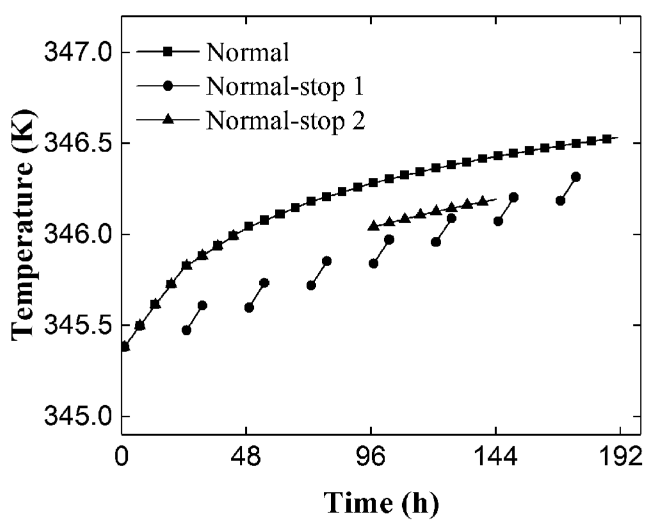

Figure 13: Variation of outlet fluid temperature under various operation schemes

Considering the variation of soil temperature in Fig. 12 and the outlet fluid temperature in Fig. 13, since the large temperature fluctuation and high outlet fluid temperature are against the heat storage, the temperature fluctuation is relatively less and the outlet temperature rising is acceptable in 192 h under the normal-stop 1 scheme. Therefore, the normal-stop 1 scheme is proposed for the vertical U-shape pipe.

4 Conclusions

The comparison of the thermal performance of two types of ETFP system was conducted numerically. The numerical method was validated and the influence factors of the shallow-buried horizontal pipe and deep-buried vertical U-shape pipe were studied. In particular, the effects of three operation schemes designed based on the actual operation conditions were analyzed and compared. The proper operation schemes were proposed for two-type ETFP system. The conclusions are as follows:

1. The boundary conditions are different in the modeling of the heat transfer process in the ETFP system with a shallow-buried horizontal pipe and a deep-buried vertical U-shape pipe. The variation of soil condition along the pipe axis direction is a key difference. The inlet velocity and ground temperature can affect the ETFP system with a shallow-buried pipe obviously. During the operation period, the fluids temperature varies smoothly compared to the system with a deep-buried vertical U-shape pipe.
2. For the ETFP system with a shallow-buried horizontal pipe, the increase of fluid velocity results in the decrease of outlet fluid temperature. The normal-stop 1 scheme has a better performance and prevents 53.1% outlet temperature rising when compared with continuous operation. The outlet fluid temperature is minimum and lower 1.2 K than it of the continuous operation after 192 h. The normal-stop 1 scheme is proposed for the horizontal ETFP system accordingly.
3. For the ETFP system with a deep-buried vertical U-shape pipe, the proper spacing is proposed to be 0.5 m. The outlet temperature rising is reduced 29.5% under normal-stop 2 when compared with continuous operation, the temperature fluctuation of soil is relatively less and rises steadily in 192 h under normal-stop 1 scheme. The normal-stop 1 scheme is also proposed for the vertical U-shape pipe.

This work focuses on the thermal performance of two-type ETFP system under different operation schemes by numerical method. Under the same conditions, the intermittent schemes have a better thermal performance than the continuous scheme. Thus, proper operation schemes are proposed for shallow-buried horizontal pipe and deep-buried vertical U-shape pipe respectively. Based on the present work, the future work will mainly study application of the ETFP system by setting pipe group including vertical and horizontal pipes, using phase change material as backfill materials and analyzing complicated moisture migration process in soils.

Funding Statement: The study is supported by the National Natural Science Foundation of China (No. 51606114) and the Science and Technology Commission of Shanghai Municipality (No. 18020501000).

Conflicts of Interest: The authors declare that they have no conflicts of interest to report regarding the present study.

References

Arvind, C.; Tiwari, G. N. (2011): A case study of a typical 2.32 kWP stand-alone photovoltaic (SAPV) in composite climate of New Delhi (India). *Applied Energy*, vol. 88, no. 4, pp. 1415-1426. DOI 10.1016/j.apenergy.2010.10.027.

Arvind, C.; Tiwari, G. N. (2010): Stand-alone photovoltaic (PV) integrated with earth to air heat exchanger (EAHE) for space heating/cooling of adobe house in New Delhi (India). *Energy Conversion and Management*, vol. 51, no. 3, pp. 393-409. DOI 10.1016/j.enconman.2009.10.001.

Babak, D. B.; Ergin, K. (2017): A new 1D analytical model for investigating the long term heat transfer rate of a borehole ground heat exchanger by Green's function method. *Renewable Energy*, vol. 108, pp. 615-621. DOI 10.1016/j.renene.2016.11.002.

Bansal, V.; Mishra, R.; Agrawal, G. D.; Mathur, J. (2012): Performance analysis of integrated earth-air-tunnel-evaporative cooling system in hot and dry climate. *Energy Buildings*, vol. 47, pp. 525-532. DOI 10.1016/j.enbuild.2011.12.024.

Bansal, V.; Misra, R.; Agrawal, G. D.; Mathur, J. (2013): Transient effect of soil thermal conductivity and duration of operation on performance of earth air tunnel heat exchanger. *Applied Energy*, vol. 103, pp. 1-11. DOI 10.1016/j.apenergy.2012.10.014.

Barakat, S.; Ramzy, A.; Hamed, A. M.; El Emam, S. H. (2016): Enhancement of gas turbine power output using earth to air heat exchanger (EAHE) cooling system. *Energy Conversion Management*, vol. 111, pp. 137-146. DOI 10.1016/j.enconman.2015.12.060.

Belatrache, D.; Bentouba, S. F.; d Bourouis, M. (2017): Numerical analysis of earth air heat exchangers at operating conditions in arid climates. *International Journal of Hydrogen Energy*, vol. 42, no. 13, pp. 8898-8904. DOI 10.1016/j.ijhydene.2016.08.221.

Bergman, T.; Lavine, A.; Incropera, F.; DeWitt, D. (2017): *Fundamentals of Heat and Mass Transfer*, pp. 81-122. 8th edition, Hoboken, NJ, USA: John Wiley & Sons Inc.

Bisoniya, T. S.; Kumar, A.; Baredar, P. (2015): Energy metrics of earth-air heat exchanger system for hot and dry climatic conditions of India. *Energy and Buildings*, vol. 86, pp. 214-221. DOI 10.1016/j.enbuild.2014.10.012.

Cui, X. G.; Zhang, J. J. (2004): Determination of the thermal influence zone of buried hot oil pipeline on steady operation. *Journal of the University of Petroleum, China*, vol. 28, no. 2, pp. 75-78 (in Chinese).

Florides, G.; Kalogirou, S. (2007): Ground heat exchangers—a review of systems, models and applications. *Renewable Energy*, vol. 32, no. 15, pp. 2461-2478. DOI 10.1016/j.renene.2006.12.014.

Fu, Z. G.; Li, L. T.; Zhang, L.; Yu, B. (2018). A numerical method and its application to investigate the thermal performance of an earth to fluid pipe system. *International Heat Transfer Conference*, vol. 16, pp. 4433-4453. Danbury, CT, USA: Begell House Inc.

Fu, Z. G.; Yu, B.; Zhu, J.; Li, W. (2012): Thaw characteristics of soil around buried pipeline in permafrost regions based on numerical simulation of temperature fields. *Journal of Thermal Science and Technology*, vol. 7, no. 1, pp. 322-333. DOI 10.1299/jtst.7.322.

Kadir, B.; Omer, O.; Kemal, C.; Omer, C. (2011): Energy analysis of a solar-ground source heat pump system with vertical closed-loop for heating applications. *Energy*, vol. 36, no. 5, pp. 3224-3232. DOI 10.1016/j.energy.2011.03.011.

Kayaci, N.; Demir, H. (2018): Numerical modelling of transient soil temperature distribution for horizontal ground heat exchanger of ground source heat pump. *Geothermics*, vol. 73, pp. 33-47. DOI 10.1016/j.geothermics.2018.01.009.

Li, G. Y.; Sheng, Y.; Jin, H. J.; Ma, W.; Qi, J. L. et al. (2010): Forecasting the oil temperatures along the proposed China-Russia crude oil pipeline using quasi 3-D transient heat conduction model. *Cold Regions Science and Technology*, vol. 64, no. 3, pp. 235-242. DOI 10.1016/j.coldregions.2009.08.003.

Liu, X.; Xiao, Y.; Inthavong, K.; Tu, J. (2015): Experimental and numerical investigation on a new type of heat exchanger in ground source heat pump system. *Energy Efficiency*, vol. 8, no. 5, pp. 845-857. DOI 10.1007/s12053-015-9324-8.

Mathur, A.; Mathur, P. S.; Agrawal, G. D.; Mathur, J. (2017): Comparative study of straight and spiral earth air tunnel heat exchanger system operated in cooling and heating modes. *Renewable Energy*, vol. 108, pp. 474-487. DOI 10.1016/j.renene.2017.03.001.

Miglani, S.; Orehounig, K.; Carmeliet, J. (2017): Design and optimization of a hybrid solar ground source heat pump with seasonal regeneration. *Energy Procedia*, vol. 122, pp. 1015-1020. DOI 10.1016/j.egypro.2017.07.468.

Miglani, S.; Orehounig, K.; Carmeliet, J. (2018): Integrating a thermal model of ground source heat pumps and solar regeneration within building energy system optimization. *Applied Energy*, vol. 218, pp. 78-94. DOI 10.1016/j.apenergy.2018.02.173.

Misra, R.; Bansal, V.; Agrawal, G. D.; Mathur, J.; Aseri, T. A. (2013): CFD analysis based parametric study of derating factor for earth air tunnel heat exchanger. *Applied Energy*, vol. 103, pp. 266-277. DOI 10.1016/j.apenergy.2012.09.041.

Ozgener, L. (2011): A review on the experimental and analytical analysis of earth to air heat exchanger (EAHE) systems in Turkey. *Renewable and Sustainable Energy Reviews*, vol. 15, no. 9, pp. 4483-4490. DOI 10.1016/j.rser.2011.07.103.

Ozgener, O.; Ozgener, L.; Tester, J. W. (2013): A practical approach to predict soil temperature variations for geothermal (ground) heat exchangers applications. *International Journal of Heat and Mass Transfer*, vol. 62, pp. 473-480. DOI 10.1016/j.ijheatmasstransfer.2013.03.031.

Pavlov, G.; Olesen, B. (2011): Seasonal solar thermal energy storage through ground heat exchangers—review of systems and applications. *Proceedings of 6th Dubrovnik Conference on Sustainable development of Energy, Water and Environmental Systems*, pp. 25-29. Dubrovnik, Croatia.

Pei, G.; Zhang, L. (2016): Heat transfer analysis of underground U-type heat exchanger of ground source heat pump system. *SpringerPlus*, vol. 5, no. 1, pp. 1863. DOI 10.1186/s40064-016-3548-8.

Ramirez-Davila, L.; Xaman, J.; Arce, J.; Alvarez, G.; Hernandez-Perez, I. (2014): Numerical study of earth-to-air heat exchanger for three different climates. *Energy and Buildings*, vol. 76, pp. 238-248. DOI 10.1016/j.enbuild.2014.02.073.

Rashidi, S.; Esfahani, J.; Karimi, N. (2018): Porous materials in building energy technologies—A review of the applications, modelling and experiments. *Renewable and Sustainable Energy Reviews*, vol. 91, pp. 229-247. DOI 10.1016/j.rser.2018.03.092.

Kepes Rodrigues, M.; da Silva Brum, R.; Vaz, J.; Oliveira Rocha, L. A.; Domingues dos Santos, E. et al. (2015): Numerical investigation about the improvement of the thermal potential of an earth-air heat exchanger (EAHE) employing the constructal design method. *Renewable Energy*, vol. 80, pp. 538-551. DOI 10.1016/j.renene.2015.02.041.

Ruiz-Calvo, F.; De Rosa, M.; Acuña, J.; Corberán, J. M.; Montagud, C. (2015): Experimental validation of a short-term Borehole-to-Ground (B2G) dynamic model. *Applied Energy*, vol. 140, pp. 210-223. DOI 10.1016/j.apenergy.2014.12.002.

Soni, S. K.; Pandey, M.; Bartaria, V. N. (2015): Ground coupled heat exchangers: a review and applications. *Renewable and Sustainable Energy Reviews*, vol. 47, pp. 83-92. DOI 10.1016/j.rser.2015.03.014.

Wang, Y.; Sun, S.; Gong, L.; Yu, B. (2018): A globally mass-conservative method for dual-continuum gas reservoir simulation. *Journal of Natural Gas Science and Engineering*, vol. 53, pp. 301-316. DOI 10.1016/j.jngse.2018.03.009.

Wang, Y.; Sun, S. Y.; Yu, B. (2017): Acceleration of gas flow simulations in dual-continuum porous media based on the mass-conservation POD method. *Energies*, vol. 10, no. 9, pp. 1-17.

Wu, X.; Liu, W.; Lu, Z. Y.; Liang, P. L.; Jin, G. (2017): Simulation on temperature variation characteristics of soil around buried pipe in process of heat storage and release. *Transactions of the Chinese Society of Agricultural Engineering*, vol. 33, no. 3, pp. 204-213 (in Chinese).

Xu, C.; Yu, B.; Zhang, Z.; Zhang, J.; Wei, J. et al. (2010): Numerical simulation of a buried hot crude oil pipeline during shutdown. *Petroleum Science*, vol. 7, no. 1, pp. 73-82. DOI 10.1007/s12182-010-0008-x.

Yu, B.; Li, C.; Zhang, Z. W.; Liu, X.; Zhang, J. J. et al. (2010): Numerical simulation of a buried hot crude oil pipeline under normal operation. *Applied Thermal Engineering*, vol. 30, no. 17-18, pp. 2670-2679. DOI 10.1016/j.applthermaleng.2010.07.016.

Zhang, L. F.; Zhang, Q.; Huang, G. S. (2016): A transient quasi-3D entire time scale line source model for the fluid and ground temperature prediction of vertical ground heat exchangers (GHEs). *Applied Energy*, vol. 170, pp. 65-75. DOI 10.1016/j.apenergy.2016.02.099.

Zhang, Z. W.; Huang, S. L.; Wang, M. Y.; Zhao, S. R. (2014): Unified heat transfer model of vertical U-tube heat exchangers for ground source heat pump system. *Engineering Mechanics*, vol. 31, pp. 269-274 (in Chinese).